

Supporting information for

$\text{Ba}_3\text{SnGa}_{10-x}\text{In}_x\text{O}_{20}$ ($0 \leq x \leq 2$): Site-selective doping, band structure
engineering and photocatalytic overall water splitting

Weihua Li, Guangxiang Lu, Yanhong Ding, Rihong Cong,* Tao Yang*

College of Chemistry and Chemical Engineering, Chongqing University, Chongqing 401331,

People's Republic of China

*Corresponding authors: congrihong@cqu.edu.cn; taoyang@cqu.edu.cn.

Table S1. Atomic coordinate, occupancy factor, isotropic thermal displacement factors for Ba₃SnGa₁₀O₂₀ obtained from Rietveld refinements

atom	site	<i>x</i>	<i>y</i>	<i>z</i>	Occ.	B _{eq}
Ba1	2a	0	0	0	1	1.20(2)
Ba2	4i	0.28026(3)	0	0.0212(1)	1	1.00(2)
Ga1	2b	0	0.5	0	0.770(4)	0.75(4)
Sn1	2b	0	0.5	0	0.230(4)	0.75(4)
Ga2	4h	0	0.36382(6)	0.5	0.615(2)	0.58(2)
Sn2	4h	0	0.36382(6)	0.5	0.385(2)	0.58(2)
Ga3	8j	0.35398(5)	0.36346(5)	0.0113(1)	1	0.72(2)
Ga4	8j	0.13874(5)	0.28522(5)	0.9758(1)	1	0.56(2)
O1	4i	0.4357(3)	0	0.8179(8)	1	0.53(3)
O2	4i	0.9018(3)	0	0.4157(8)	1	0.53(3)
O3	8j	0.2384(2)	0.3645(3)	0.8988(6)	1	0.53(3)
O4	8j	0.4143(2)	0.2501(2)	0.8400(6)	1	0.53(3)
O5	8j	0.8610(2)	0.1446(2)	0.8640(6)	1	0.53(3)
O6	8j	0.0739(2)	0.3797(3)	0.1801(6)	1	0.53(3)

$a = 15.19472(3) \text{ \AA}$, $b = 11.76213(3) \text{ \AA}$, $c = 5.15730(1) \text{ \AA}$, $\beta = 90.9765(1) \text{ \AA}$, $V = 921.591(3) \text{ \AA}^3$

$R_p = 3.211\%$, $R_{wp} = 4.221\%$, $R_{exp} = 2.156\%$, $GOF = 1.958$.

Definition of R factors and GOF:

$$R_p = \frac{\sum |Y_{o,m} - Y_{c,m}|}{\sum Y_{o,m}} \quad R_{wp} = \left[\frac{\sum w_m (Y_{o,m} - Y_{c,m})^2}{\sum w_m Y_{o,m}^2} \right]^{1/2}$$

$$R_{exp} = \left[\frac{(N-P)}{\sum w_m Y_{o,m}^2} \right]^{1/2} \quad GOF = R_{wp} / R_{exp}$$

Table S2. Selected metal-oxygen bond distances (Å) for Ba₃SnGa_{10-x}In_xO₂₀ (0 ≤ x ≤ 2.0) obtained from Rietveld refinements

Bond	x = 0	x = 0.5	x = 1.0	x = 1.5	x = 2.0
M1-O1 × 2	1.923(4)	1.853(6)	1.984(5)	2.002(6)	1.904(8)
M1-O6 × 4	2.022(3)	2.037(4)	2.052(3)	2.066(4)	2.146(6)
<M1-O>	1.989	1.976	2.029	2.045	2.065
M2-O1 × 2	2.091(3)	2.124(4)	2.165(3)	2.220(4)	2.210(5)
M2-O4 × 2	2.033(3)	2.104(4)	2.088(3)	2.136(4)	2.190(6)
M2-O6 × 2	2.020(3)	2.037(4)	2.113(3)	2.153(4)	2.147(6)
<M2-O>	2.048	2.088	2.122	2.170	2.182
Ga3-O2 × 1	1.834(2)	1.831(3)	1.832(2)	1.841(3)	1.826(4)
Ga3-O3 × 1	1.841(3)	1.862(4)	1.798(3)	1.802(4)	1.866(6)
Ga3-O4 × 1	1.852(3)	1.838(4)	1.834(3)	1.821(4)	1.847(6)
Ga3-O5 × 1	1.823(3)	1.768(4)	1.811(3)	1.800(4)	1.738(6)
<Ga3-O>	1.838	1.825	1.819	1.816	1.819
Ga4-O3 × 1	1.828(3)	1.854(4)	1.859(3)	1.858(4)	1.923(6)
Ga4-O4 × 1	1.852(3)	1.812(4)	1.869(3)	1.855(4)	1.782(6)
Ga4-O5 × 1	1.848(3)	1.860(4)	1.857(3)	1.869(4)	1.899(6)
Ga4-O6 × 1	1.831(3)	1.843(4)	1.806(3)	1.802(4)	1.795(6)
<Ga4-O>	1.840	1.842	1.848	1.846	1.850

Table S3. Atomic coordinate, occupancy factor, isotropic thermal displacement factors for $\text{Ba}_3\text{SnGa}_9.5\text{In}_{0.5}\text{O}_{20}$ obtained from Rietveld refinements

atom	site	x	y	z	Occ.	B_{eq}
Ba1	2a	0	0	0	1	1.49(3)
Ba2	4i	0.27982(5)	0	0.0188(1)	1	1.19(2)
Ga1	2b	0	0.5	0	0.656(5)	0.98(5)
Sn1/In1	2b	0	0.5	0	0.344(5)	0.98(5)
Ga2	4h	0	0.36130(7)	0.5	0.422(2)	0.81(3)
Sn2/In2	4h	0	0.36130(7)	0.5	0.578(2)	0.81(3)
Ga3	8j	0.35296(7)	0.36508(7)	0.0096(2)	1	0.95(3)
Ga4	8j	0.13967(7)	0.28434(7)	0.9744(2)	1	0.54(3)
O1	4i	0.4396(4)	0	0.807(1)	1	0.50(5)
O2	4i	0.9010(4)	0	0.411(1)	1	0.50(5)
O3	8j	0.2377(3)	0.3676(4)	0.8866(8)	1	0.50(5)
O4	8j	0.4105(3)	0.2536(3)	0.8323(8)	1	0.50(5)
O5	8j	0.8587(3)	0.1473(3)	0.8491(7)	1	0.50(5)
O6	8j	0.0734(3)	0.3781(4)	0.1779(8)	1	0.50(5)

$a = 15.26409(4) \text{ \AA}$, $b = 11.81621(3) \text{ \AA}$, $c = 5.18857(1) \text{ \AA}$, $\beta = 90.9007(2) \text{ \AA}$, $V = 935.715(5) \text{ \AA}^3$

$R_p = 4.184\%$, $R_{\text{wp}} = 5.492\%$, $R_{\text{exp}} = 2.498\%$, $\text{GOF} = 2.199$.

Table S4. Atomic coordinate, occupancy factor, isotropic thermal displacement factors for $\text{Ba}_3\text{SnGa}_9\text{InO}_{20}$ obtained from Rietveld refinements

atom	site	x	y	z	Occ.	B_{eq}
Ba1	2a	0	0	0	1	1.22(2)
Ba2	4i	0.27980(4)	0	0.0175(1)	1	0.97(2)
Ga1	2b	0	0.5	0	0.535(4)	0.46(4)
Sn1	2b	0	0.5	0	0.465(4)	0.46(4)
Ga2	4h	0	0.35937(5)	0.5	0.233(2)	0.70(2)
Sn2	4h	0	0.35937(5)	0.5	0.767(2)	0.70(2)
Ga3	8j	0.35242(5)	0.36477(5)	0.0093(2)	1	0.56(2)
Ga4	8j	0.14077(5)	0.28291(5)	0.9768(2)	1	0.48(2)
O1	4i	0.4324(3)	0	0.8218(9)	1	0.45(4)
O2	4i	0.9008(3)	0	0.4175(9)	1	0.45(4)
O3	8j	0.2406(2)	0.3645(3)	0.8997(6)	1	0.45(4)
O4	8j	0.4125(2)	0.2557(3)	0.8357(6)	1	0.45(4)
O5	8j	0.8582(2)	0.1447(3)	0.8557(6)	1	0.45(4)
O6	8j	0.0763(2)	0.3776(3)	0.1681(7)	1	0.45(4)

$a = 15.32033(4) \text{ \AA}$, $b = 11.85491(3) \text{ \AA}$, $c = 5.21515(1) \text{ \AA}$, $\beta = 90.8105(2) \text{ \AA}$, $V = 947.086(4) \text{ \AA}^3$

$R_p = 3.140\%$, $R_{\text{wp}} = 4.092\%$, $R_{\text{exp}} = 2.220\%$, $\text{GOF} = 1.844$.

Table S5. Atomic coordinate, occupancy factor, isotropic thermal displacement factors for $\text{Ba}_3\text{SnGa}_{8.5}\text{In}_{1.5}\text{O}_{20}$ obtained from Rietveld refinements

atom	site	x	y	z	Occ.	B_{eq}
Ba1	2a	0	0	0	1	1.19(3)
Ba2	4i	0.27946(5)	0	0.0154(1)	1	0.85(2)
Ga1	2b	0	0.5	0	0.330(4)	0.36(4)
Sn1	2b	0	0.5	0	0.670(4)	0.36(4)
Ga2	4h	0	0.35732(6)	0.5	0.085(2)	0.70(2)
Sn2	4h	0	0.35732(6)	0.5	0.915(2)	0.70(2)
Ga3	8j	0.35190(6)	0.36516(6)	0.0089(2)	1	0.47(2)
Ga4	8j	0.14198(6)	0.28126(6)	0.9759(2)	1	0.23(3)
O1	4i	0.4296(4)	0	0.819(1)	1	0.33(4)
O2	4i	0.9021(3)	0	0.421(1)	1	0.33(4)
O3	8j	0.2405(3)	0.3643(3)	0.8980(8)	1	0.33(4)
O4	8j	0.4113(3)	0.2595(3)	0.8296(7)	1	0.33(4)
O5	8j	0.8584(2)	0.1438(3)	0.8513(7)	1	0.33(4)
O6	8j	0.0767(3)	0.3759(3)	0.1618(8)	1	0.33(4)

$a = 15.37493(5) \text{ \AA}$, $b = 11.89386(4) \text{ \AA}$, $c = 5.24437(2) \text{ \AA}$, $\beta = 90.6945(2)^\circ$, $V = 958.954(6) \text{ \AA}^3$

$R_p = 3.518\%$, $R_{\text{wp}} = 4.563\%$, $R_{\text{exp}} = 2.253\%$, $\text{GOF} = 2.025$.

Table S6. Atomic coordinate, occupancy factor, isotropic thermal displacement factors for Ba₃SnGa₈In₂O₂₀ obtained from Rietveld refinements

atom	site	<i>x</i>	<i>y</i>	<i>z</i>	Occ.	B _{eq}
Ba1	2a	0	0	0	1	1.63(5)
Ba2	4i	0.27884(7)	0	0.0127(2)	1	1.09(3)
Ga1	2b	0	0.5	0	0	1.19(5)
Sn1	2b	0	0.5	0	1	1.19(5)
Ga2	4h	0	0.35566(8)	0.5	0	0.97(3)
Sn2	4h	0	0.35566(8)	0.5	1	0.97(3)
Ga3	8j	0.35226(9)	0.36605(9)	0.0061(3)	1	0.68(4)
Ga4	8j	0.1434(1)	0.28000(9)	0.9729(3)	1	0.14(4)
O1	4i	0.4375(6)	0	0.810(2)	1	0.56(7)
O2	4i	0.8997(6)	0	0.414(2)	1	0.56(7)
O3	8j	0.2395(4)	0.3724(5)	0.874(1)	1	0.56(7)
O4	8j	0.4100(4)	0.2609(5)	0.814(1)	1	0.56(7)
O5	8j	0.8569(4)	0.1456(5)	0.835(1)	1	0.56(7)
O6	8j	0.0778(4)	0.3696(5)	0.166(1)	1	0.56(7)

$a = 15.41431(8) \text{ \AA}$, $b = 11.93819(6) \text{ \AA}$, $c = 5.27206(3) \text{ \AA}$, $\beta = 90.5704(3) \text{ \AA}$, $V = 970.112(9) \text{ \AA}^3$

$R_p = 5.302\%$, $R_{wp} = 7.049\%$, $R_{exp} = 2.250\%$, $GOF = 3.134$.

Table S7. Bond valences sum of In^{3+} and Sn^{4+} located at M1 or M2 site in $\text{Ba}_3\text{SnGa}_{10-x}\text{In}_x\text{O}_{20}$

($0 \leq x \leq 2.0$)

$x = 0$				
	In1	In2	Sn1	Sn2
Bond valence sum	/	/	4.821	4.091
$x = 0.5$				
	In1	In2	Sn1	Sn2
Bond valence sum	5.060	3.645	5.102	3.674
$x = 1.0$				
	In1	In2	Sn1	Sn2
Bond valence sum	4.269	3.323	4.304	3.350
$x = 1.5$				
	In1	In2	Sn1	Sn2
Bond valence sum	4.094	2.924	4.127	2.948
$x = 2.0$				
	In1	In2	Sn1	Sn2
Bond valence sum	4.058	2.820	4.091	2.843

Table S8. Estimated band gap energy for $\text{Ba}_3\text{SnGa}_{10-x}\text{In}_x\text{O}_{20}$

$\text{Ba}_3\text{SnGa}_{10-x}\text{In}_x\text{O}_{20}$	E_g/eV
$x = 0$	4.53
$x = 0.5$	4.50
$x = 1.0$	4.47
$x = 1.5$	4.41
$x = 2.0$	4.27

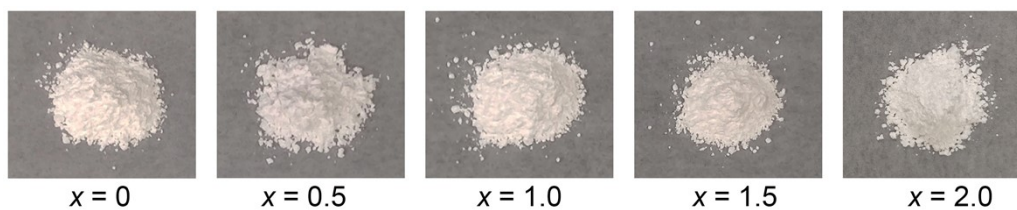


Fig. S1. Photographs of $\text{Ba}_3\text{SnGa}_{10-x}\text{In}_x\text{O}_{20}$ ($0 \leq x \leq 2.0$) samples.

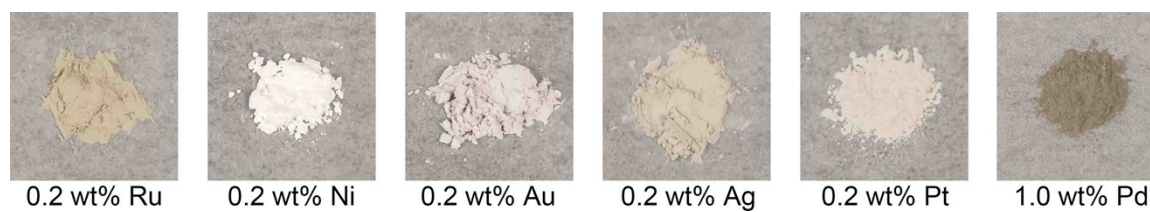


Fig. S2. Photographs for $\text{Ba}_3\text{SnGa}_{8.5}\text{In}_{1.5}\text{O}_{20}$ loaded with different cocatalysts.

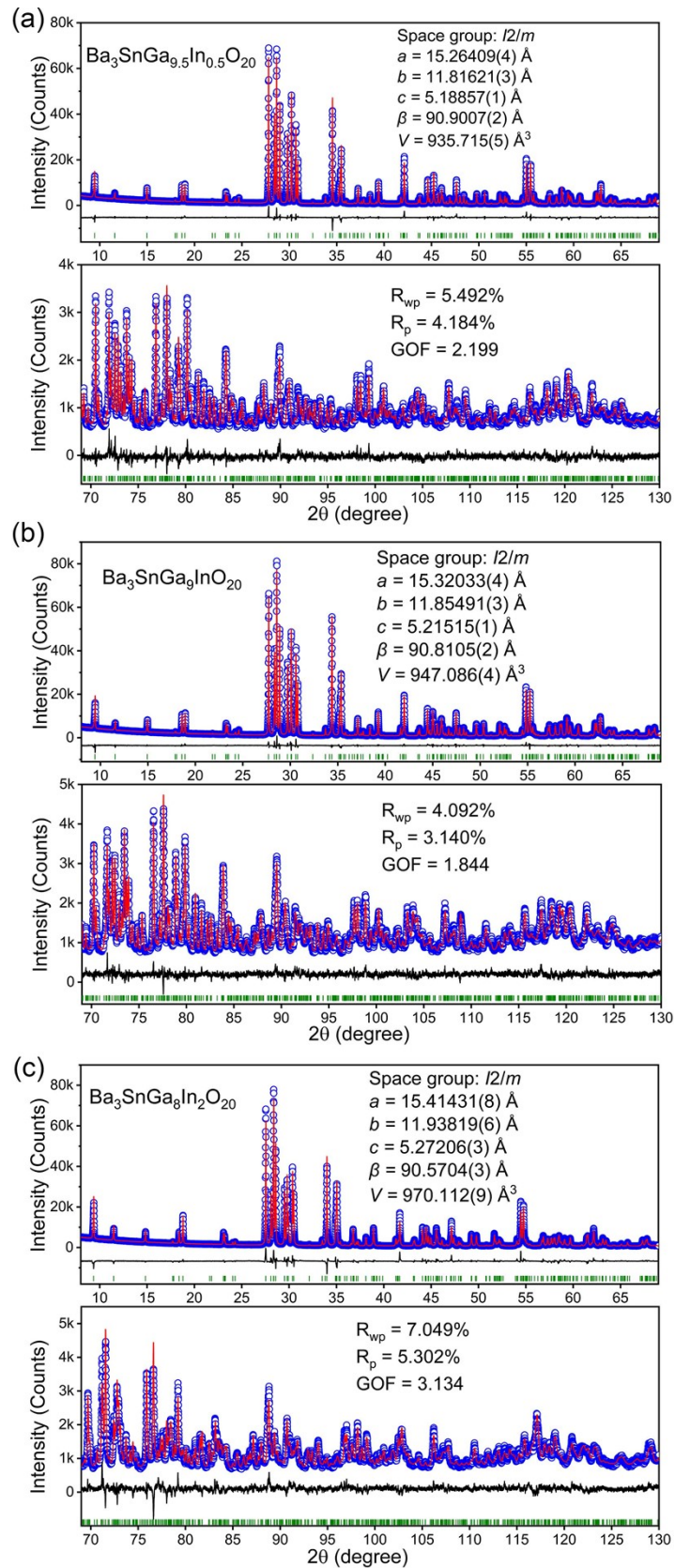


Fig. S3. Final convergence of the Rietveld refinements on high quality powder X-ray diffraction data for (a) $\text{Ba}_3\text{SnGa}_{9.5}\text{In}_{0.5}\text{O}_{20}$, (b) $\text{Ba}_3\text{SnGa}_9\text{InO}_{20}$, (c) $\text{Ba}_3\text{SnGa}_8\text{In}_2\text{O}_{20}$.

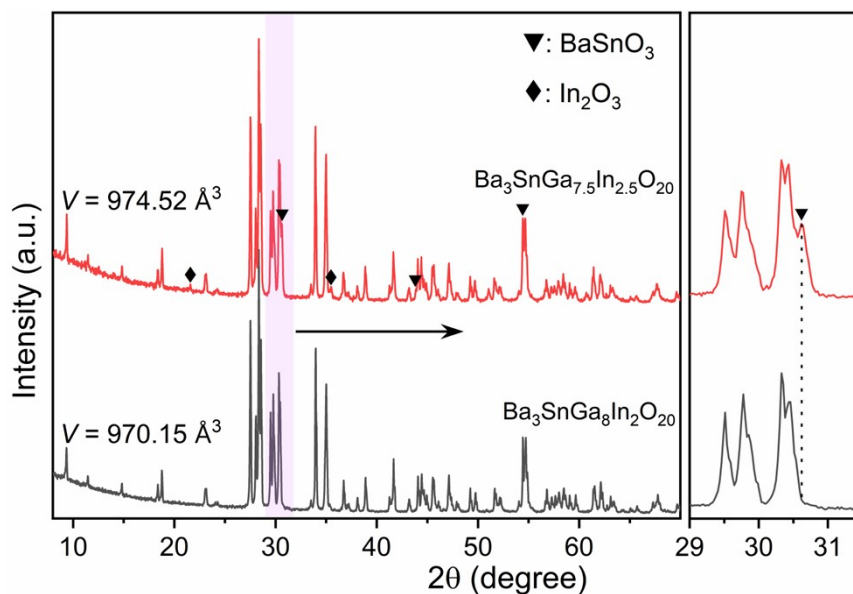


Fig. S4. Powder XRD patterns for phase-pure $\text{Ba}_3\text{SnGa}_8\text{In}_2\text{O}_{20}$ (gray line) and impure $\text{Ba}_3\text{SnGa}_{7.5}\text{In}_{2.5}\text{O}_{20}$ (red line). The impurity phases can be identified as BaSnO_3 and In_2O_3 .

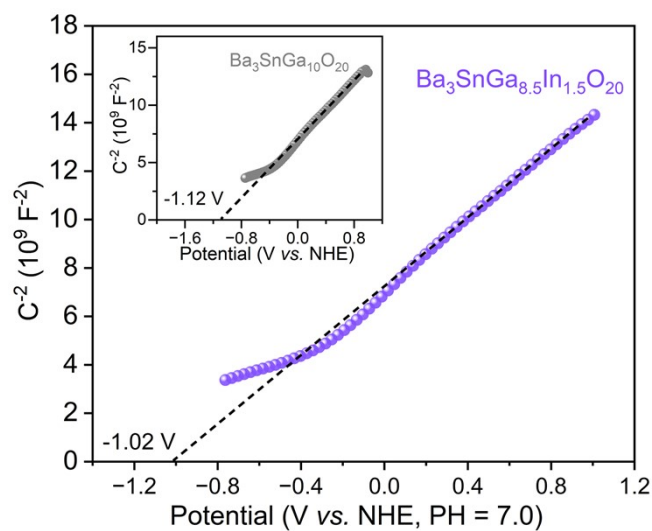


Fig. S5. Mott-Schottky plots for $\text{Ba}_3\text{SnGa}_{10}\text{O}_{20}$ (the inset) and $\text{Ba}_3\text{SnGa}_{8.5}\text{In}_{1.5}\text{O}_{20}$ in a 0.3 M Na_2SO_4 aqueous solution (pH = 7.0).

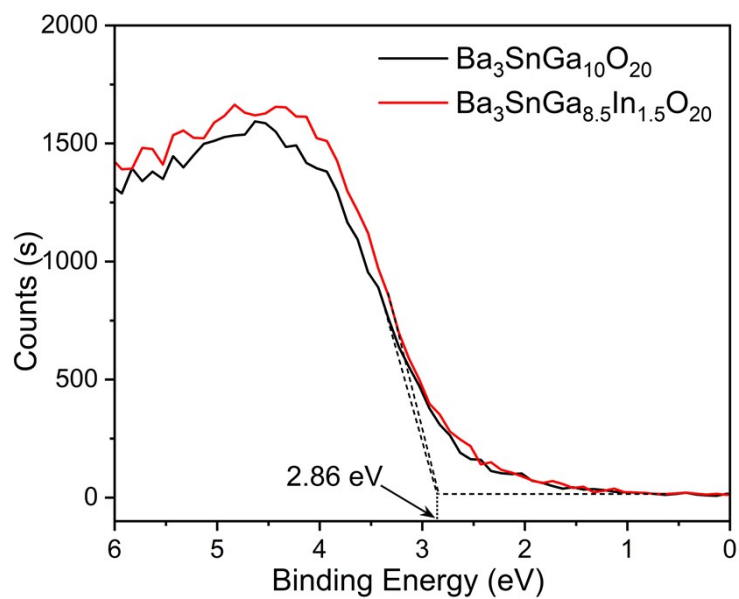


Fig. S6. Valence band-XPS curves for $\text{Ba}_3\text{SnGa}_{10-x}\text{In}_x\text{O}_{20}$ ($x = 0, 1.5$).

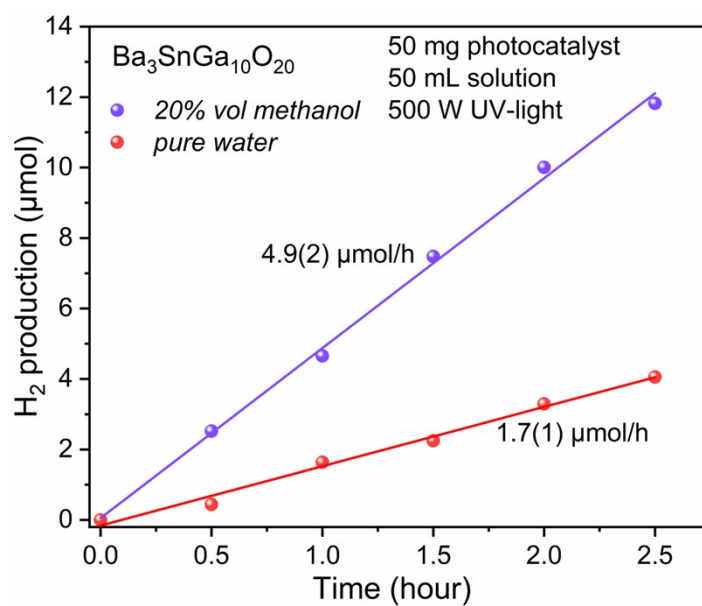


Fig. S7. Photocatalytic H_2 generation of $\text{Ba}_3\text{SnGa}_{10}\text{O}_{20}$ in 20 vol.% methanol aqueous solution (blue line) and in pure water (red line), respectively.

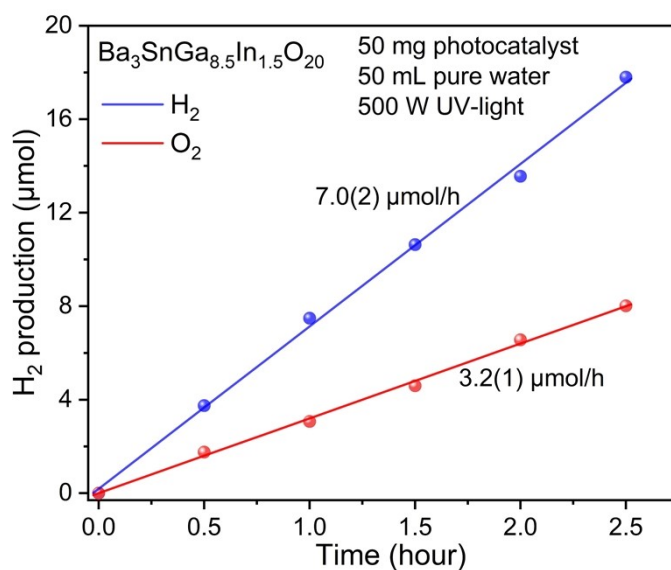


Fig. S8. Photocatalytic H₂ (blue line) and O₂ (red line) generation for Ba₃SnGa_{8.5}In_{1.5}O₂₀ in pure water.

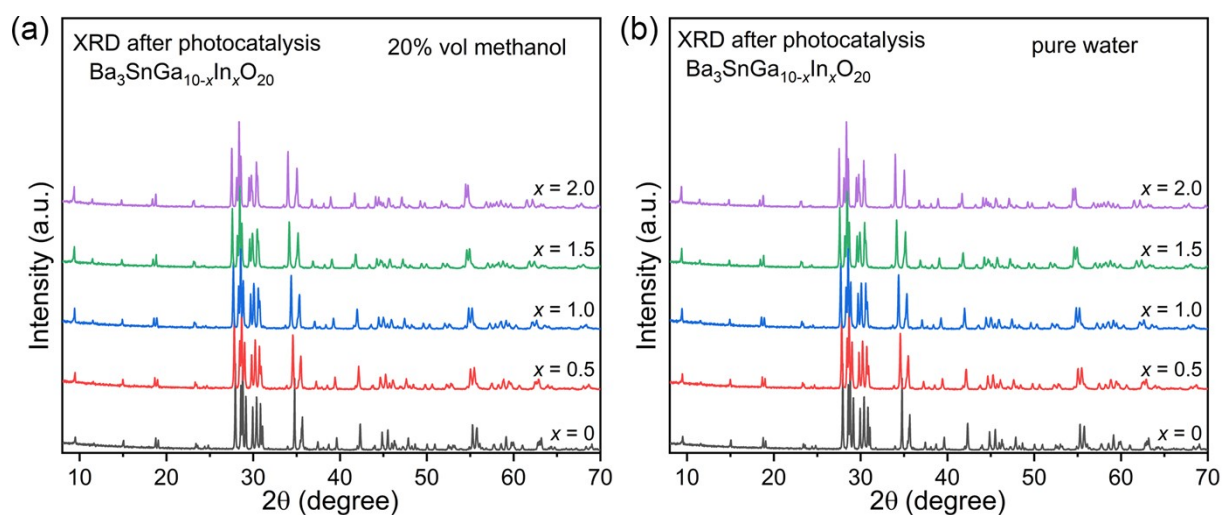


Fig. S9. Powder XRD patterns for Ba₃SnGa_{10-x}In_xO₂₀ ($0 \leq x \leq 2$) after photocatalytic reaction (a) in 20 vol.% methanol aqueous solution and (b) in pure water, respectively.

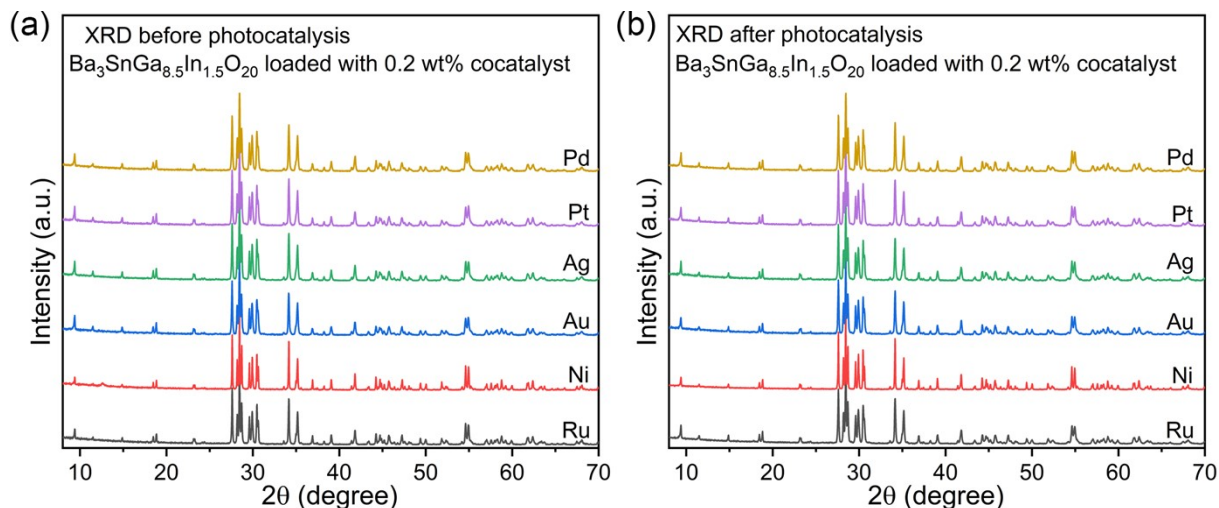


Fig. S10. Powder XRD patterns (a) before and (b) after photocatalytic reactions for $\text{Ba}_3\text{SnGa}_{8.5}\text{In}_{1.5}\text{O}_{20}$ loaded with various cocatalysts.

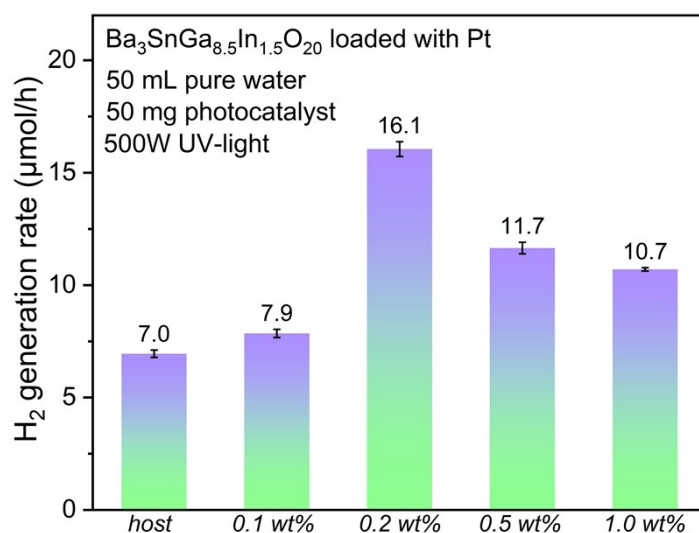


Fig. S11. Photocatalytic H_2 generation rates for $\text{Ba}_3\text{SnGa}_{8.5}\text{In}_{1.5}\text{O}_{20}$ loaded with different amounts of Pt.

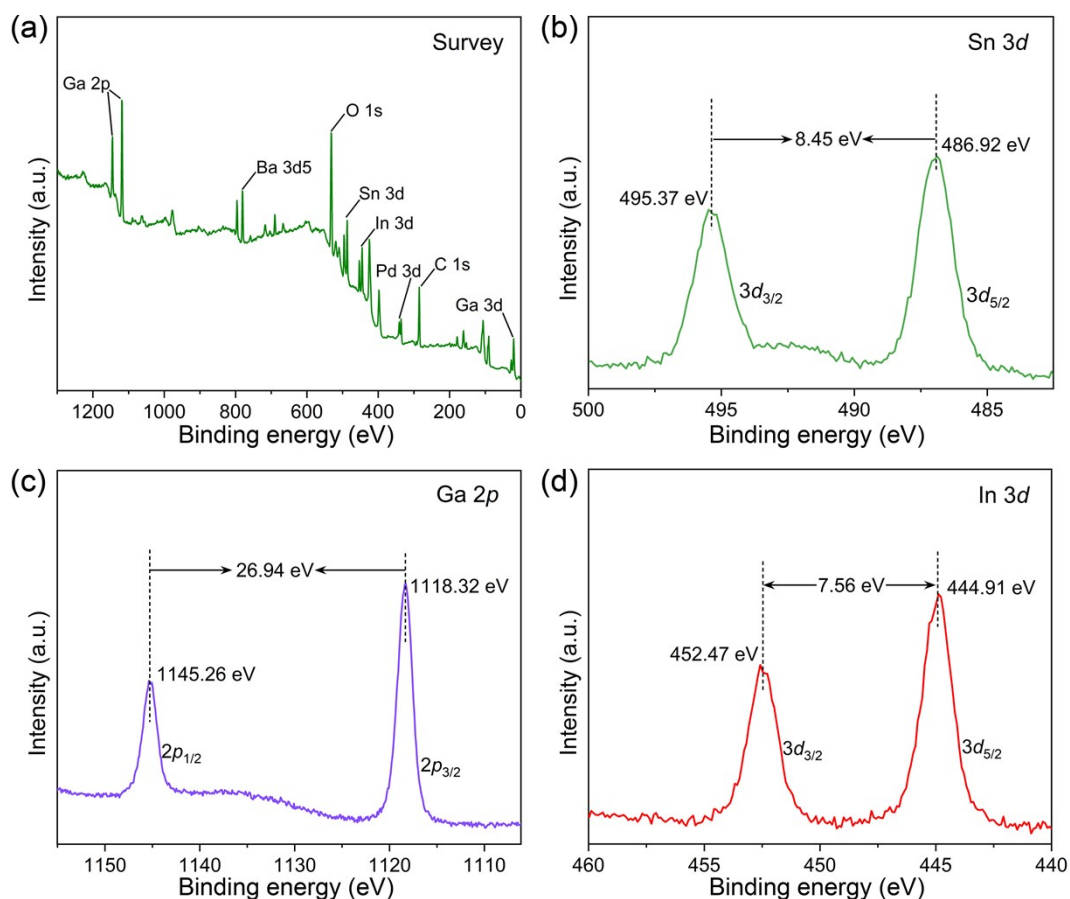


Fig. S12. (a) XPS survey scan of $\text{Ba}_3\text{SnGa}_{8.5}\text{In}_{1.5}\text{O}_{20}$ loaded with 1 wt% Pd; (b) Sn 3d, (c) Ga 2p and (d) In 3d XPS spectra.

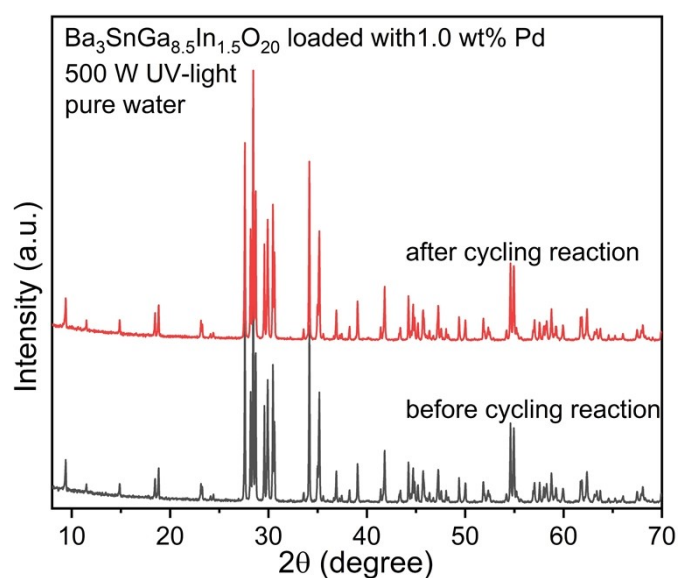


Fig. S13. Powder XRD patterns before (gray line) and after (red line) cyclic photocatalytic overall water splitting for $\text{Ba}_3\text{SnGa}_{8.5}\text{In}_{1.5}\text{O}_{20}$ loaded with 1.0 wt% Pd.

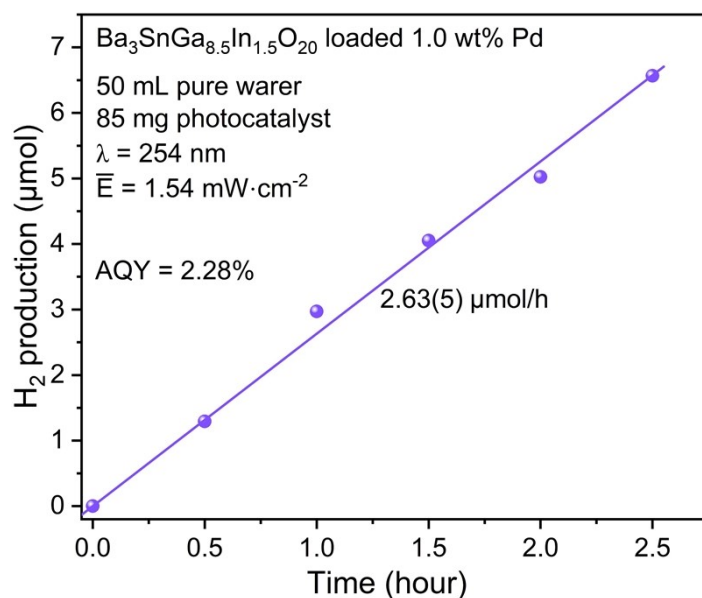


Fig. S14. Photocatalytic H₂ generation curve for Ba₃SnGa_{8.5}In_{1.5}O₂₀ loaded with 1.0 wt% Pd. Photocatalytic condition: 85 mg of photocatalyst; 50 mL pure water; 500 W mercury lamp equipped with a 254 nm bandpass filter.

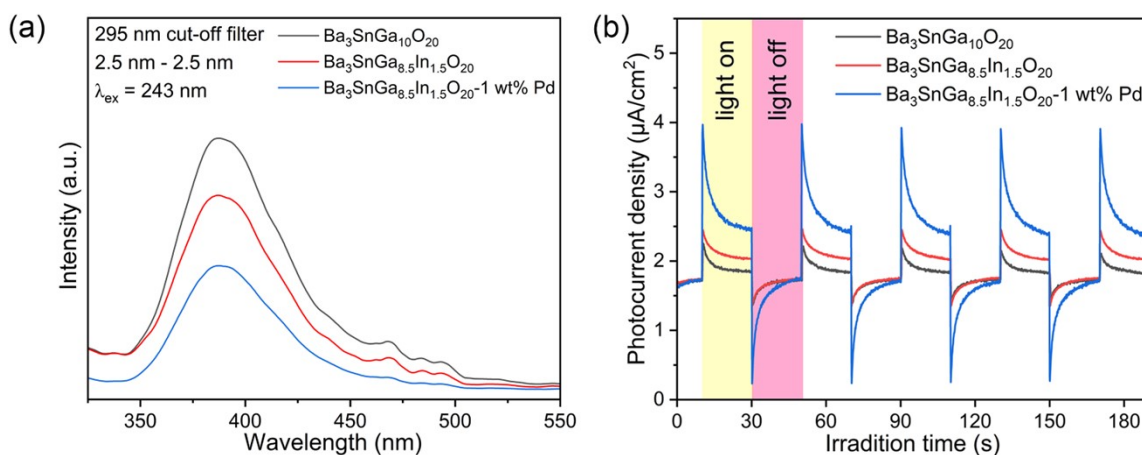


Fig. S15. (a) PL emission spectra and (b) transient photocurrent responses for Ba₃SnGa₁₀O₂₀ (gray lines), Ba₃SnGa_{8.5}In_{1.5}O₂₀ (red lines), and Ba₃SnGa_{8.5}In_{1.5}O₂₀ loaded with 1.0 wt% Pd (blue lines), respectively.